Goulding, W, Sun, Y and Ashley, J

NanoMIP Beacons with a Co-operative Binding Mechanism for the all-in-one Detection of Methamphetamine Aptamer Complexes

Journal Pre-proof

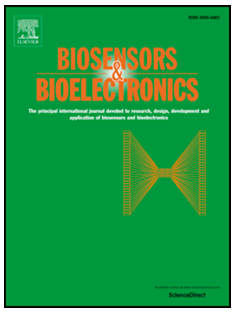

NanoMIP Beacons with a Co-operative Binding Mechanism for the all-in-one Detection of Methamphetamine Aptamer Complexes

William Goulding, Yi Sun, Jon Ashley

PII: S0956-5663(24)00863-7

DOI: https://doi.org/10.1016/j.bios.2024.116856

Reference: BIOS 116856

To appear in: *Biosensors and Bioelectronics*

Received Date: 10 July 2024

Revised Date: 10 September 2024

Accepted Date: 13 October 2024

Please cite this article as: Goulding, W., Sun, Y., Ashley, J., NanoMIP Beacons with a Co-operative Binding Mechanism for the all-in-one Detection of Methamphetamine Aptamer Complexes, *Biosensors and Bioelectronics*, https://doi.org/10.1016/j.bios.2024.116856.

NanoMIP Beacons with a Co-operative Binding Mechanism for the all-in-one Detection of Methamphetamine Aptamer Complexes

William Goulding[a], Yi Sun[b] and Jon Ashley[a]*

[a]Forensic Research Institute (FORRI), School of Pharmaceutical and Biomolecular Sciences, Liverpool John Moores University, 3 Byrom Way, Liverpool L3 3AF,

[b]Technical University of Denmark, Department of Health Technology, Kgs. Lyngby 2800, Denmark; telephone number: +44(0)151 231 2998, email: j.ashley@ljmu.ac.uk

Abstract

Methamphetamine is a highly addictive stimulant with significant public health implications, necessitating the development of rapid, sensitive, and reliable detection methods. Traditional analytical techniques, though accurate, often involve complex sample preparation, expensive equipment, and lengthy analysis times. This study presents the design, synthesis, and application of nanoMIP beacons with a unique co-operative binding mechanism for the detection of methamphetamine. NanoMIP beacons selective for methamphetamine/aptamer complexes were synthesized using a solid-phase synthesis method that involved the bio-conjugation of an aptamer on the stationary phase and the incubation of methamphetamine to form a methamphetamine-aptamer complex. The resultant nanoMIP beacons were eluted off the affinity column and characterised using transmission electron microscopy. The co-operative binding mechanism, which relies on the structure-switching capability of the aptamer upon analyte binding was demonstrated through comparison of the fluorescence quenching signal of a scrambled sequence and nanoNIP controls. The fluorescence quenching assay was established using a fixed optimal concentration of aptamer and varying amounts of methamphetamine. The nanoMIP beacons showed enhanced the sensitivity (LOD = 23 ± 3.5 nM) and excellent selectivity, with a 40-fold increase in quenching for methamphetamine compared to other illicit drugs. The nanoMIP beacons demonstrated acceptable sample recoveries in both urine diluent and 50% human serum. This work provides a new strategy

for the development of hybrid nanoMIP/aptamer-based sensors and provides a robust analytical tool for combating methamphetamine abuse.

Keywords

Aptamers, Molecularly Imprinted Polymers, nanoMIP, Methamphetamine, Forensic Science, Stimulants

1 Introduction

Methamphetamine is a potent central nervous system stimulant that poses significant public health challenges worldwide due to its high potential for abuse and addiction (Cohen-Laroque et al., 2024). The illicit production, distribution, and consumption of methamphetamine has led to a pressing need for rapid, sensitive, and reliable detection methods. Traditional analytical techniques such as gas chromatography-mass spectrometry (GC-MS) and liquid chromatography-mass spectrometry (LC-MS) are highly accurate but often require complex sample preparation, expensive equipment, and lengthy analysis times (Bickel et al., 2024; Deng et al., 2020). Consequently, there is a growing interest in developing portable and cost-effective biosensors for the detection of stimulants such as methamphetamine in various settings, including forensic, clinical, and environmental applications (Bano et al., 2023).

Two common types of bio-recognition elements utilised in biosensors for the detection of stimulants are molecularly imprinted polymers (MIPs) and aptamers(Ashley et al., 2017; Naseri et al., 2020). NanoMIPs have been demonstrated in a number of electrochemical sensors as recognition elements for the detection of both amphetamine and 3,4-Methyl enedioxymethamphetamine (MDMA); (F. Truta et al., 2023; F. M. Truta et al., 2023), while aptamers which specifically bind to methamphetamine, have been applied in electrochemical and fluorescence-based sensors for the detection of methamphetamine (Chang et al., 2024; Wang et al., 2024).

The combined use of MIPs and aptamers has emerged as a promising area of biosensing and combines the advantages of both types of bio-recognition element such as the ease of engineering both nanoMIPs and aptamers with different functionalities such as fluorophores and quenchers (Bossi et al., 2023; Qiao et al., 2021). In addition, the combined use of aptamers and nanoMIPs can serve to enhance the total binding and introduce non-natural interactions such as hydrophobic interactions which, only contribute a small amount of the total binding interactions in an aptamer.

Most attempts to develop hybrid MIP aptamers to date, have all focused on incorporating aptamers as monomers into MIPs through the use of a polymerizable moiety on the aptamer either on the DNA base group (Poma et al., 2015) or at the 5′ or 3′ terminal ends of the aptamer (Zhang and Liu, 2019; Zhou et al., 2022).

The combined use of aptamers and MIPs was first described by Wei Bai et. al for the detection of thrombin whereby the 3′ and 5′ terminal ends of the aptamer were modified with polymerizable moieties and incorporated into hydrogels (Bai et al., 2013). In 2021, Sullivan et al. demonstrated the combined use of molecularly imprinted polymers and aptamers for the recognition of trypsin and moxifloxacin (Sullivan et al., 2021b, 2021a). The thymine base groups of a trypsin selective aptamer were chemically modified with a polymerizable moiety to allow for the aptamer to be fully integrated into the MIP recognition site, although this strategy may detrimentally affect the binding of the aptamer as typically base groups are involved in the binding interactions between the aptamer and target.

Other strategies for the incorporation of aptamers into MIPs include immobilisation of the aptamers onto biosensor surfaces through bio-conjugation followed by surface imprinting (Ali and El-Wekil, 2023) or through self-assembly of the aptamer and the non-covalent encapsulation of the aptamer during polymerisation (Geng et al., 2018). Recently, researchers have demonstrated the use of aptamer/MIP hybrids to detect leptin by firstly immobilising a previously published aptamer sequence to a gold NPs/Pt NSs modified surface (Erkmen et

al., 2023). The MIP was then generated by incubating leptin with the aptamer to form the complex and forming a MIP film via electro-polymerisation on the electrode. Turk et al. recently reported the use of a multiwalled carbon nanotube (MWCNT)/aptamer/molecularly imprinted polymer (MIP)-Based Biosensor for the detection of thrombin (Turk et al., 2024). Little attention has been given to imprinting ssDNA aptamers as templates in their own right, through non-covalent imprinting. The use of dsDNA, as a template may not be practical due to the lack of variation in the 3D structure that a double helix would offer and would be insufficient to give sequence specific recognition. Aptamers on the other hand can form unique 3D structures based on their sequence making them and their complexes viable as templates for imprinting. In addition, with the use of capture SELEX or trial and error truncation, aptamers with structural switching capability (changes its 3D conformation upon binding the target from the unbound state) can be developed (Feagin et doubt, 2018).

In this manuscript, we present the design, synthesis, and application of nanoMIP beacons with a unique co-operative binding mechanism for the all-in-one detection of methamphetamine/aptamer complexes (**Figure 1A**). NanoMIP beacons were synthesized using solid-phase synthesis through a bio-conjugation of the aptamer on the stationary phase and incubation of methamphetamine to form a methamphetamine aptamer complex. The synthesized nanoMIP beacons were characterised and evaluated for morphology, signal transduction and assay performance demonstrated in the simulated urine samples and human serum samples.

By harnessing the power of structure switching aptamers whereby the 3D conformation of the aptamer changes upon binding of the analyte and synthesizing the nanoMIP beacon to recognise the 3D conformation of the aptamer in its bound state, we demonstrated that our nanoMIP beacons bind via a co-operative binding mechanism for the rapid and efficient detection of methamphetamine. This work not only contributes to the advancement of both

nanoMIP and hybrid nanoMIP/DNA based sensors but also addresses a critical need in public health and safety by providing a robust analytical tool for combating methamphetamine abuse.

2 Materials and Methods

2.1 Materials and Chemicals

The methamphetamine aptamer was taken from a previously published sequence which was truncated with structural switching capability as demonstrated through dichroism spectroscopy (Xie et al., 2022). Both the aptamer and scrambled sequence were purchased from IDT with the following sequences respectively /5AmMC6/CGG TTG CAA GTG GGA CTC TGG TAG GCT GGG TTA ATT TG/3BHQ_1/ and /5AmMC6/GGC AGG TGT GTG ATT GTT AGT CGG TAA CAT TCG AGC GGT G/3BHQ_1/, where /5AmMC6 is the amino group and /3BHQ_1/ is a black hole quencher. For the functionalisation of the glass beads, N- Potters; Spheriglass A glass 2429 CP-00 was purchased from Silmid (UK) . 3-Glycidyloxypropyl) trimethoxysilane (GPTMS) and toluene were purchased from Sigma-Aldrich. For the nanoMIP synthesis, N-Isopropylacrylamide (NIPAm), N-tert-butylacrylamide (TBA), acrylic acid (Acc), fluorescein o-acrylate, N-(3-aminopropyl)methacrylamide HCl (APM), and N,N′-methylenebis(acrylamide) (BIS) were used as the monomers and cross-linker, while ammonium persulfate (APS) and N,N,N′,N′-tetramethylethylenediamine (TEMED) were used as the initiator and catalyst, respectively, and were all purchased from Sigma-Aldrich. Drug standards for Amphetamine, MDMA, ketamine, morphine, codeine and methadone were used in house. All sample recoveries were performed using urine diluent and 50% human serum purchased from Sigma Aldrich.

All fluorescence quenching experiments were performed on a Tecan Synergy plate reader using black 96 well plates at an excitation wavelength (λ_{ex}) of 465 nm and emission range

between 500 and 610 nm as well as a gain of 80. The band width was kept at 20 nm. Transmission electron microscopy (TEM) images were taken on a FEI Morgagni transmission electron microscope.

2.2 Functionalisation of Glass Beads with the Methamphetamine Aptamer

70 g of glass beads were washed with 1 M NaOH prior to use, washed with water until the pH was neutralised and dried. The glass beads were incubated with 2 % (3-Glycidyloxypropyl)trimethoxysilane (GPTMS) in anhydrous toluene at 55 ^{o}C for 48 hrs. The resultant epoxide functionalised glass beads were washed with 8 x 30 ml volumes of acetone and dried under vacuum. The resultant glass beads were then incubated with 10 μM of methamphetamine aptamer in carbonate buffer pH 9.0 overnight. The unreacted epoxide groups were blocked with 1mM ethanolamine. The resultant aptamer functionalised glass beads were washed with 8 x 30 ml volumes of water and stored in 50 mM tris buffer pH 7.4. at 4^{o}C to ensure that all non-conjugated aptamer is removed.

2.3 Synthesis of Methamphetamine/Aptamer complex Selective nanoMIP Beacons.

Using a modified version of the chemically initiated solid-phase imprinting technique (Canfarotta et al., 2016), 70 g of glass beads were incubated with 10 mM of methamphetamine in 50 mM tris buffer pH 7.4 for 1 hour to form the aptamer methamphetamine complex. The solution was then removed using vacuum and the difference between the absorbance before and after incubation was measured on a UV spectrometer to confirm the formation of the complex. 100 ml pre-polymerisation mixture containing NIPAm (0.34 mmol), ACC (0.032 mmol), TBAm (0.26 mmol), BIS (0.013 mmol), N-(3-aminopropyl)methacrylamide HCl (APM) (0.06 mmol), fluorescein o-acrylate (1.29 μmol) and 10 μM methamphetamine in 50 mM tris buffer pH 7.4 was degassed by bubbling nitrogen for 30- 60 minutes. 20 ml of this pre-polymerisation was then percolated onto the glass beads and incubated. The polymerization

was initiated by the addition of TEMED (30 µl) followed by 500 µl of 0.13 mmol APS. The reaction was left for 16 hours with overhead stirring. The glass beads were washed with 8-bed volumes of DI water to remove the unreacted monomers and reagents and low affinity nanoMIP beacons and methamphetamine nanoMIPs. The high affinity nanoMIP beacons were eluted by incubating the glass beads in pre-warmed water (60 ^{o}C) and the glass bead SPE column was incubated in a water bath set at 60 ^{o}C for 15 minutes. The nanoMIP beads were then eluted via vacuum pump and manifold. The elution was repeated two more times. The final nanoMIPs were stored at 4 ^{o}C until further use. A non-imprinted control (nanoNIP) beacon was synthesized in the same manner as the nanoMIP beacon with the aptamer conjugated glass beads but in the absence of methamphetamine during the incubation with step and in the pre-polymerisation mixture. The absence of leeched methamphetamine was confirmed using UV absorption. The glass beads were regenerated by incubating the glass beads in water for 2 - 4 hrs before washing with 10 x 30 ml DI water.

2.4 Characterisation of nanoMIP Beacons.

The resultant nanoMIP beacons were characterised by TEM by depositing 10 µl of nanoMIP beacons onto formvar coated TEM grids and dried overnight. The fluorescence signal of the nanoMIP was confirmed by scanning the fluorescence signal of the resultant nanoMIP beacons.

The extent of non-specific quenching of nanoMIP beacons caused by the aptamer in the absence of methamphetamine was determined by incubating 50 µl of nanoMIP beacon with 50 µl of either the methamphetamine aptamer or scrambled sequence (SS) at different concentrations (0.001 to 10 µM) in 50 mM tris buffer pH 7.4 . The extent of binding was also determined for the positive control nanoNIP beacon by incubating 50 µl of nanoNIP beacon with 50 µl of either the methamphetamine aptamer different concentrations (0.001 to 10 µM) in 50 mM Tris buffer pH 7.4 and the fluorescence scan was taken.

2.5 Fluorescence Quenching Assay

Fluorescence quenching assays were performed by mixing (100 nM, 1 μM and 5 μM) of methamphetamine aptamer or SS with 1 ml (0.25 mg /ml) of nanoMIP beacon in 50 mM Tris buffer pH 7.4. 50 μl of this solution was incubated with different concentrations of methamphetamine (0.1 to 10 μM) and the fluorescence scan/fluorescence intensity was measured. The extent of fluorescence quenching was determined using the Stern-Volmer equation by plotting the ratio $[(I_o/I) - 1]$ against methamphetamine concentration. Subsequent fluorescence quenching assays were performed by premixing 5 μM aptamer ligand with the nanoMIP beacons. The Stern-Volmer constant was found to be K_{SV} = 0.0005370 nM^{-1} for the nanoMIP beacons.

The selectivity of the sensor was determined by incubating premixing 5 μM of methamphetamine aptamer or SS with 1 ml of nanoMIP beacon in 50 mM tris buffer pH 7.4. 50 μl of this solution was incubated with the highest concentration of each illicit drug (10 μM) and the extent of fluorescence quenching was measured from the $[(I_o/I) - 1]$ ratio.

2.6 NanoMIP Beacon Performance in Real Samples.

The ability of the nanoMIP beacons to detect methamphetamine in urine diluent was performed by determining the sample recoveries of methamphetamine in the presence of the aptamer ligand and nanoMIP beacon. Sample recoveries were performed by premixing 5 μM of methamphetamine aptamer or SS with 1 ml of nanoMIP beacon in 50 mM Tris buffer pH 7.4. 50 μl of this solution was incubated with spiked concentrations of methamphetamine (30, 60, 500 and 1250 nM) in urine diluent or human serum and compared to the unspiked sample. Fluorescence measurements were performed, and the fluorescence quenching was determined from the Stern-Volmer ratio $[(I_o/I) - 1]$. The found concentrations were

determined by extrapolation of the Stern-Volmer ratio from the linear Stern-Volmer plot and the unspiked sample was assumed to be zero.

3. Results and Discussion

3.1 Functionalisation of Glass Beads.

In this study, we utilised the solid phase synthesis technique for the production of nanoMIP beacons against the methamphetamine/aptamer complex. Attempts to imprint biological complexes have been previously described by Ambrosini et. al. who demonstrated the molecular imprinting of a trypsin/p-aminobenzamidine complex using the solid-phase technique however, the binding properties of the nanoMIP against the complex was never characterise (Ambrosini et al., 2013). As observed with other types of template (Kalecki et al., 2020), the solid-phase imprinting technique along with surface imprinting allows for the aptamers to be fixed into the same orientation through conjugation of the 3′ terminal amino group through nucleophilic reaction with an epoxide group on the surface of the glass beads. The use of solid-phase imprinting also allows for the nanoMIP beacons to be easily washed to remove unreacted monomers and separate the nanoMIP beacons from the methamphetamine aptamer complex template through a hot elution. Also, it is worth noting that the methamphetamine cannot be immobilized itself due to the lack of functional groups for bio-conjugation.

The functionalisation of the glass beads with the methamphetamine aptamer and formation of the methamphetamine aptamer complex were confirmed using a native gel and UV absorbance spectroscopy respectively. **Figure 1B** shows the native gel before and after incubation with the aptamer. The decrease in the intensity of the aptamer band after incubation with the glass beads confirms that most of the aptamer was attached to the glass beads. The formation of the methamphetamine/aptamer complex was confirmed by a

decrease in absorbance of the supernatant collected after incubation when compared to an aliquot taken before incubation. The pre-polymerisation mixture also contains methamphetamine in excess to ensure the complexes are maintained throughout imprinting. Any formation of nanoMIPs against the free methamphetamine template can easily be removed through washing the column. The pre-polymerisation mixture was also buffered in Tris buffer at 7.4 pH to avoid hydrolysis of the DNA aptamer at low pH by acrylic acid. Initial attempts to synthesize nanoMIPs beacons utilised both the chemically initialised and the living photo-polymerisation techniques (Poma et al., 2014, 2013). However, the photo-polymerisation method was found to cause photobleaching of the fluorophore. It was also suspected that the aptamer degrades in the presence of the UV light making the photo-polymerisation method incompatible with DNA based templates. Going forward, the chemical polymerisation was used for all subsequent batches of nanoMIP beacons.

3.2 Characterisation of the nanoMIP Beacons

The resultant nanoMIPs were characterised by TEM (**Figure 1C**). Particles were found to have round morphologies and an average diameter of about 100 nm. The measurement of the hydrodynamic radius of the nanoMIP beacons via dynamic light scattering was not possible due to the interference from the fluorophore in the measurements. Average yield from the chemical polymerisation was estimated to be 0.21 mg/g^{-1} glass beads based on the cumulative amount of freeze dried nanoMIP beacons.

The fluorescence signal and co-operative binding mechanism of the nanoMIP was recorded and optimised on the Tecan plate reader. The effect of different concentrations of the methamphetamine aptamer ligand on the fluorescence quenching of nanoMIP beacons (**Figure 2A**) and corresponding scrambled sequence control (SS) (**Figure 2B**) in the absence of the methamphetamine analyte showed that the methamphetamine aptamer and scrambled sequence displayed only a slight quenching/binding effect even at concentrations up to 10

μM, which is suspected to be due to either dynamic quenching or artifact quenching. The effect of different concentrations of methamphetamine aptamer ligands on the fluorescence of the nanoNIP beacon control synthesized in the absence of methamphetamine (**Figure 2C**) showed a high quenching effect towards the methamphetamine aptamer which demonstrates that it is possible to molecularly imprint an aptamer based on its 3D conformation and the difference in quenching comes down to the nanoMIP beacon being able to recognise and bind the methamphetamine complex while the nanoNIP is able to recognise the aptamer in its unbound 3D conformation.

These results confirm that the methamphetamine aptamer complex was imprinted successfully and the methamphetamine aptamer ligand and analyte must undergo structure switching upon binding to each other for signal transduction to occur. The strong fluorescence quenching effect of the nanoNIP beacon control suggests that molecular recognition sites are formed on the basis of the aptamer's 3D folding conformation, which is dictated by the sequence of aptamer and the ionic strength and buffer conditions.

Next, the effect of methamphetamine concentration with a fixed concentration of methamphetamine aptamer (100, 1000 and 5000 nM respectively) on the extent of fluorescence quenching of the nanoMIP beacons were determined. The degree of fluorescence quenching was plotted against the methamphetamine as shown in **figure 3A.** As the concentration of methamphetamine aptamer is increased, the degree of fluorescence quenching also increased with an increasing concentration of methamphetamine. As the K_D was previously reported as 79.62 nM (Wang et al., 2024), the dynamic range of the nanoMIP beacon is limited when the aptamer concentration is near to the K_D value. These results suggest that the dynamic range of the sensor can be tuned if required so that the dynamic range and the expected levels of analyte can be matched. A fixed aptamer concentration of 5 μM was selected for all subsequent experiments. The effect of the amount of fluorescein methacrylate (0-10 umol) on the

quenching of the nanoMIP beacons were also determined and is shown in Figure 3B. At concentrations above 10 μmol a little to no quenching is observed due to the saturation of fluorescein methacrylate monomers being incorporated into the nanoMIP beacon. As the monomer concentration decreases, there is an observed increase in fluorescence quenching with the optimum amount being 1.29 μmol. Below this concentration we start to see a rapid loss of fluorescence signal and hence quenching is limited.

3.2 Development of nanoMIP Beacon Assay.

We then demonstrated the effect of methamphetamine concentration on the fluorescence quenching of the nanoMIP beacons incubated at a fixed concentration of 5 μM of the methamphetamine aptamer ligand or SS respectively (**Figure 4A-C**). Comparing the extent of quenching of the nanoMIP beacons between the methamphetamine aptamer ligand and SS, it can be seen that in the presence of the methamphetamine aptamer, an increasing dose dependent fluorescence quenching signal is observed for the nanoMIP beacons which reaches a saturation at concentrations over 2000 nM. In contrast, the SS gives rise to a slight decrease in fluorescence signal through quenching of the nanoMIP beacons when incubated with increasing concentrations of methamphetamine. Any change in fluorescence could be due to dynamic quenching of the SS with the nanoMIP.

Taking the linear concentration range of the assay for both the methamphetamine aptamer and SS control, the corresponding linear Stern-Volmer calibration plots (**Figure 4D**) were plotted. The minimum performance criteria of the fluorescence were determined for the assay. The dynamic range of the nanoMIP beacons were determined to be between 34 - 1200 nM and the limit of detection (LOD) was determined from the stand deviation of 5 blank samples. The LOD was determined to be 23 ± 3.5 nM in optimal buffer conditions.

The selectivity of the nanoMIP beacons were determined by incubating 10 μM of each drug candidate with a fixed concentration of 5 μM of fixed aptamer or SS respectively with the nanoMIP beacons (**Figure 5**). The degree of quenching was found to be at least 40 X higher for methamphetamine compared to the other drug candidates, namely, amphetamine, MDMA, Codeine morphine, methadone and ketamine, suggesting excellent selectivity of nanoMIP beacons towards methamphetamine with little cross-reactivity of the aptamer towards these other drug targets. The slight quenching observed for both the methamphetamine aptamer and SS for other drugs could be due to dynamic quenching.

The sample recoveries were determined to test the effect of two of two different samples matrices, namely urine diluent and human serum on the nanoMIP beacon assay. The nanoMIP beacons were incubated with different spiked concentrations of methamphetamine (34, 60, 500 and 1200 nM) with a fixed concentration of 5 μM of aptamer ligand in 100% urine diluent and 50 % human serum (**Table 1**). NanoMIP beacons showed spiked recoveries in urine diluent varied from 113.3 to 95.4 % (RSD: 1.9 to 4.2 %) while the sample recoveries in 50 % human serum varied from 112.7 to 97.9 % (RSD: 3.3 to 0.18 %) demonstrating acceptable recoveries for both sample types.

4. Conclusion

In this manuscript, we demonstrated the first application of nanoMIP beacons for the detection of methamphetamine. Using solid-phase imprinting, we were able to successfully demonstrate the molecular imprinting of a methamphetamine aptamer complex with an average size of about 100 nm. The conjugation of the aptamer allows for the control of the orientation of the quencher on the 3' end, allows us to form the methamphetamine aptamer complex and facilities easy washing and elution of the nanoMIP beacons off the column. Due to the structural switching ability of the aptamer, we were able to demonstrate signal transduction through a unique co-operative biorecognition mechanism by comparing the

nanoMIP beacons and methamphetamine aptamer ligand with the scrambled sequence and nanoNIP controls. The nanoMIP beacons demonstrated excellent sensitivity in the nanomolar detection limits. The dynamic range of the sensor was demonstrated to be tuneable and modulated by the aptamer concentration with an aptamer concentration of 5 μM being the optimal concentration used for each assay. The nanoMIP beacons demonstrated excellent selectivity showing a 40 x selectivity towards methamphetamine. The unique co-operative binding mechanism demonstrated by nanoMIP beacons serves to reduced non-specific binding of the nanoMIPs with minimal sample preparation as demonstrated by the sample recoveries in urine diluent. This proof-of-concept can potentially allow for any analyte to be detected as an alternative to ELISA based immunoassays provided that the aptamer can demonstrate structural switching capability or in the case of proteins and other macromolecules, rely on a size difference between the complex and aptamer on its own. Currently, we are looking at expanding this sensor platform for the detection of other types of analytes such as proteins and other small molecules.

Funding Sources

The authors would like to acknowledge the support and funding of a CAMS Fellowship [Grant number: 600310/22/06] from the Analytical Chemistry Trust Fund' and 'Community for Analytical Measurement Science' for funding.

References

Ali, R., El-Wekil, M.M., 2023. A dual-recognition-controlled electrochemical biosensor for selective and ultrasensitive detection of acrylamide in heat-treated carbohydrate-rich food. Food Chem 413. https://doi.org/10.1016/j.foodchem.2023.135666

Ambrosini, S., Beyazit, S., Haupt, K., Tse Sum Bui, B., 2013. Solid-phase synthesis of molecularly imprinted nanoparticles for protein recognition. Chemical Communications 49, 6746–6748. https://doi.org/10.1039/c3cc41701h

Ashley, J., Shahbazi, M.A., Kant, K., Chidambara, V.A., Wolff, A., Bang, D.D., Sun, Y., 2017. Molecularly imprinted polymers for sample preparation and biosensing in food analysis: Progress and perspectives. Biosens Bioelectron 91, 606–615. https://doi.org/10.1016/j.bios.2017.01.018

Bai, W., Gariano, N.A., Spivak, D.A., 2013. Macromolecular amplification of binding response in superaptamer hydrogels. J Am Chem Soc 135, 6977–6984. https://doi.org/10.1021/ja400576p

Bano, H., Suleman, S., Anzar, N., Parvez, S., Narang, J., 2023. A review on advancement of biosensors for the detection of amphetamine drug. Int J Environ Anal Chem 00, 1–29. https://doi.org/10.1080/03067319.2023.2229747

Bickel, J., Szewczyk, A., Aboutara, N., Jungen, H., Müller, A., Ondruschka, B., Iwersen-Bergmann, S., 2024. Chiral analysis of amphetamine, methamphetamine, MDMA and MDA enantiomers in human hair samples. J Anal Toxicol 226–234. https://doi.org/10.1093/jat/bkae026

Bossi, A.M., Marinangeli, A., Quaranta, A., Pancheri, L., Maniglio, D., 2023. Time-Resolved Fluorescence Spectroscopy of Molecularly Imprinted Nanoprobes as an Ultralow Detection Nanosensing Tool for Protein Contaminants. Biosensors (Basel) 13. https://doi.org/10.3390/bios13070745

Canfarotta, F., Poma, A., Guerreiro, A., Piletsky, S., 2016. Solid-phase synthesis of molecularly imprinted nanoparticles. Nat Protoc 11, 443–455. https://doi.org/10.1038/nprot.2016.030

Chang, W., Zheng, Z., Ma, Y., Du, Y., Shi, X., Wang, C., 2024. An electrochemical aptasensor for methylamphetamine rapid detection by single-on mode based on competition with complementary DNA. Sci Rep 14, 1–12. https://doi.org/10.1038/s41598-024-59505-6

Cohen-Laroque, J., Grangier, I., Perez, N., Kirschner, M., Kaiser, S., Sabé, M., 2024. Positive and negative symptoms in methamphetamine-induced psychosis compared to schizophrenia: A systematic review and meta-analysis. Schizophr Res 267, 182–190. https://doi.org/10.1016/j.schres.2024.03.037

Deng, Y., Guo, C., Zhang, H., Yin, X., Chen, L., Wu, D., Xu, J., 2020. Occurrence and removal of illicit drugs in different wastewater treatment plants with different treatment techniques. Environ Sci Eur 32. https://doi.org/10.1186/s12302-020-00304-x

Erkmen, C., Aydoğdu Tig, G., Uslu, B., 2023. Evaluation of aptamer and molecularly imprinted polymers as a first hybrid sensor for leptin detection at femtogram levels. Talanta 265. https://doi.org/10.1016/j.talanta.2023.124809

Feagin, T.A., Maganzini, N., Soh, H.T., 2018. Strategies for Creating Structure-Switching Aptamers. ACS Sens 3, 1611–1615. https://doi.org/10.1021/acssensors.8b00516

Geng, Y., Guo, M., Tan, J., Huang, S., Tang, Y., Tan, L., Liang, Y., 2018. A fluorescent molecularly imprinted polymer using aptamer as a functional monomer for sensing of kanamycin. Sens Actuators B Chem 268, 47–54. https://doi.org/10.1016/j.snb.2018.04.065

Kalecki, J., Iskierko, Z., Cieplak, M., Sharma, P.S., 2020. Oriented Immobilization of Protein Templates: A New Trend in Surface Imprinting. ACS Sens 5, 3710–3720. https://doi.org/10.1021/acssensors.0c01634

Naseri, M., Mohammadniaei, M., Sun, Y., Ashley, J., 2020. The use of aptamers and molecularly imprinted polymers in biosensors for environmental monitoring: A tale of two receptors. Chemosensors. https://doi.org/10.3390/CHEMOSENSORS8020032

Poma, A., Brahmbhatt, H., Pendergraff, H.M., Watts, J.K., Turner, N.W., 2015. Generation of novel hybrid aptamer-molecularly imprinted polymeric nanoparticles. Advanced Materials 27, 750–758. https://doi.org/10.1002/adma.201404235

Poma, A., Guerreiro, A., Caygill, S., Moczko, E., Piletsky, S., 2014. Automatic reactor for solid-phase synthesis of molecularly imprinted polymeric nanoparticles (MIP NPs) in water. RSC Adv 4, 4203–4206. https://doi.org/10.1039/c3ra46838k

Poma, A., Guerreiro, A., Whitcombe, M.J., Piletska, E. V., Turner, A.P.F., Piletsky, S.A., 2013. Solid-Phase Synthesis of Molecularly Imprinted Polymer Nanoparticles with a Reusable Template-"Plastic Antibodies". Adv Funct Mater 23, 2821–2827. https://doi.org/10.1002/adfm.201202397

Qiao, Q., Guo, X., Wen, F., Chen, L., Xu, Q., Zheng, N., Cheng, J., Xue, X., Wang, J., 2021. Aptamer-Based Fluorescence Quenching Approach for Detection of Aflatoxin M1 in Milk. Front Chem 9, 1–8. https://doi.org/10.3389/fchem.2021.653869

Sullivan, M. V., Allabush, F., Bunka, D., Tolley, A., Mendes, P.M., Tucker, J.H.R., Turner, N.W., 2021a. Hybrid aptamer-molecularly imprinted polymer (AptaMIP) nanoparticles selective for the antibiotic moxifloxacin. Polym Chem 12, 4394–4405. https://doi.org/10.1039/d1py00607j

Sullivan, M. V., Clay, O., Moazami, M.P., Watts, J.K., Turner, N.W., 2021b. Hybrid Aptamer-Molecularly Imprinted Polymer (aptaMIP) Nanoparticles from Protein Recognition—A Trypsin Model. Macromol Biosci 21. https://doi.org/10.1002/mabi.202100002

Truta, F., Garcia Cruz, A., Tertis, M., Zaleski, C., Adamu, G., Allcock, N.S., Suciu, M., Ștefan, M.G., Kiss, B., Piletska, E., De Wael, K., Piletsky, S.A., Cristea, C., 2023. NanoMIPs-based electrochemical sensors for selective detection of amphetamine. Microchemical Journal 191. https://doi.org/10.1016/j.microc.2023.108821

Truta, F.M., Cruz, A.G., Dragan, A.M., Tertis, M., Cowen, T., Stefan, M.G., Topala, T., Slosse, A., Piletska, E., Van Durme, F., Kiss, B., De Wael, K., Piletsky, S.A., Cristea, C., 2023. Design of smart nanoparticles for the electrochemical detection of 3,4-methylenedioxymethamphetamine to allow in field screening by law enforcement officers. Drug Test Anal 1–14. https://doi.org/10.1002/dta.3605

Turk, F., Atilgan, A., Yildirim-Tirgil, N., 2024. Sensitive and Selective Electrochemical Determination of Thrombin as a Peptide Biomarker by a Multiwalled Carbon Nanotube (MWCNT)/Aptamer/Molecularly Imprinted Polymer (MIP)-Based Biosensor. Anal Lett 57, 383–396. https://doi.org/10.1080/00032719.2023.2209678

Wang, Y., Wang, Z., Tong, Y., Zhang, D., Yun, K., Yan, J., Niu, W., 2024. Aptamer-based fluorescent sensor for highly sensitive detection of methamphetamine. Luminescence 39. https://doi.org/10.1002/bio.4687

Xie, Y., Wu, S., Chen, Z., Jiang, J., Sun, J., 2022. Rapid nanomolar detection of methamphetamine in biofluids via a reagentless electrochemical aptamer-based biosensor. Anal Chim Acta 1207. https://doi.org/10.1016/j.aca.2022.339742

Zhang, Z., Liu, J., 2019. Molecular Imprinting with Functional DNA. Small 15, 1–12. https://doi.org/10.1002/smll.201805246

Zhou, Q., Xu, Z., Liu, Z., 2022. Molecularly Imprinting–Aptamer Techniques and Their Applications in Molecular Recognition. Biosensors (Basel) 12. https://doi.org/10.3390/bios12080576

Figure Captions

Figure 1: nanoMIP beacons with a unique co-operative binding signal transduction (A), native gel of aptamer before (1) and after (2) incubation with glass beads (B) and TEM images of nanoMIP beacons (C).

Figure 2 Extent of fluorescence quenching of nanoMIP beacons when incubated with different concentrations of methamphetamine aptamer ligand (A), SS (B) respectively. The extent of fluorescence quenching of nanoNIP beacons with different concentrations of the methamphetamine aptamer ligand only (C); Plot of fluorescence vs aptamer concentration for the aptamer/nanoMIP beacon, SS/nanoMIP beacon and aptamer nanoMIP beacons (D).

Figure 3 The effect of different methamphetamine (0-10000 nM) on the fluorescence quenching of nanoMIP beacons at different fixed concentrations of methamphetamine aptamer ligand (100 nM, 1000 nM and 5000 nM) (A); The effect of fluorescein methacyrlate amount (1.29 – 10 μmol) on the quenching of nanoMIP beacons in the presence of 5000 nM aptamer and methamphetamine (0 - 1200 nM) (B).

Figure 4 Extent of fluorescence quenching of the nanoMIP beacons in the presence of a fixed concentration of methamphetamine aptamer (A) and scrambled sequence (SS) and methamphetamine (0 – 10 μM) (B); The extent of fluorescence quenching of nanoMIP beacons with different concentrations of methamphetamine (C) and the corresponding Stern-Volmer calibration plots (n =3).

Figure 5 Fluorescence quenching response of nanoMIP beacons when incubated with 5 μM of aptamer or SS and 10000 nM of each drug (methamphetamine, amphetamine, MDMA, codeine, morphine, methadone, and ketamine) respectively as well as 5 μM of aptamer or SS (n=3).

Table Captions

Table 1 spiked recoveries of nanoMIP beacons in urine diluent and 50 % human serum samples (n =3).

Table 1

Urine Diluent			
Spiked concentration	**Observed concentration**	**Recovery %**	**RSD %**
30 nM	**34 ± 1.23 nM**	**113**	**2.8**
500 nM	**525 ± 0.67 nM**	**105**	**4.2**
1200 nM	**1143 ± 0.72 nM**	**95.4**	**1.9**
50 % Human Serum			
Spiked concentration	**Observed concentration**	**Recovery %**	**RSD %**
60 nM	**67.7 ± 2.28 nM**	**113**	**3.3**
500 nM	**542 ± 5.86 nM**	**108**	**1.1**
1200 nM	**1224 ± 2.21 nM**	**97.9**	**0.18**

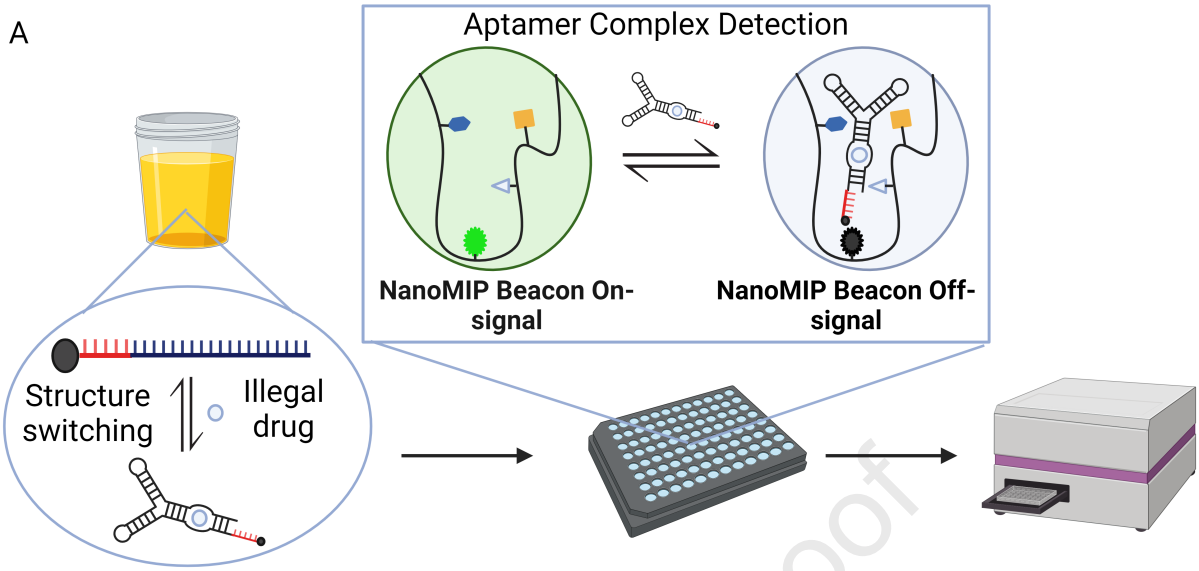

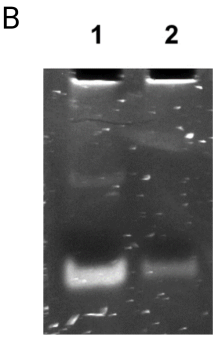

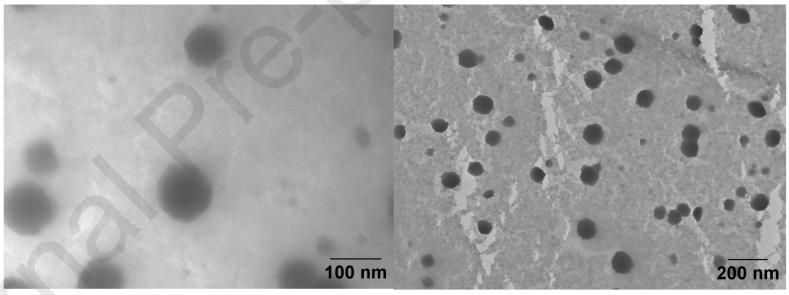

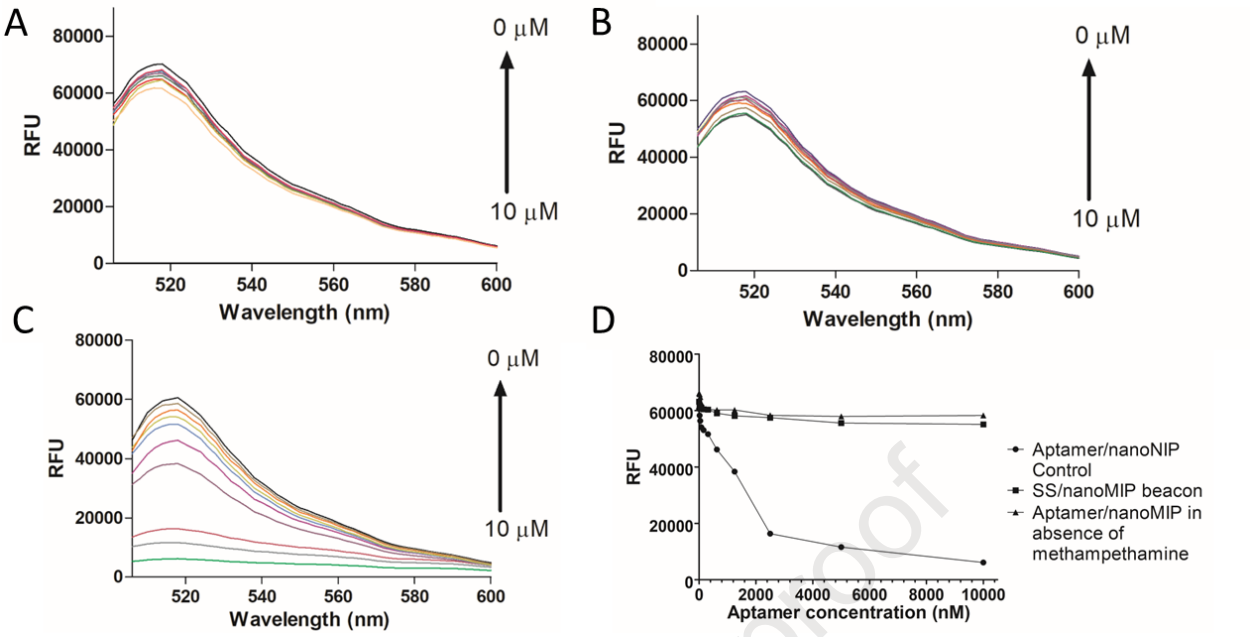

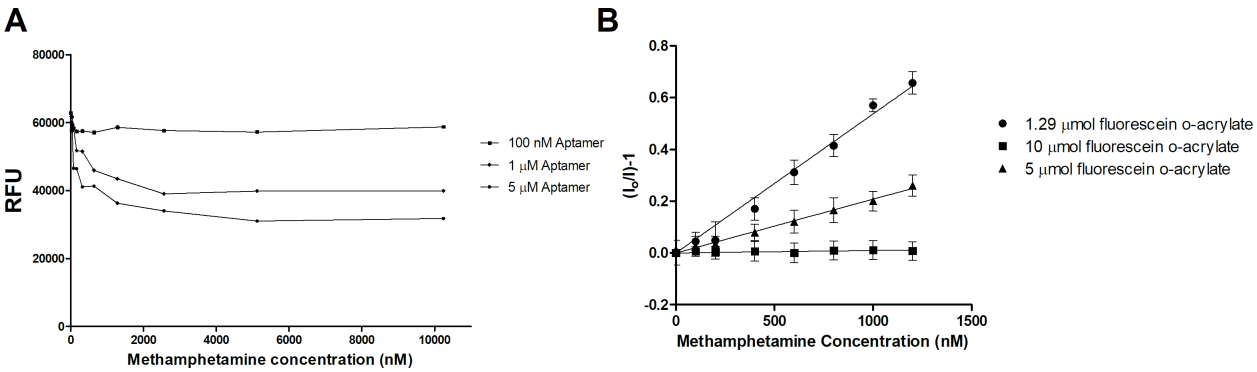

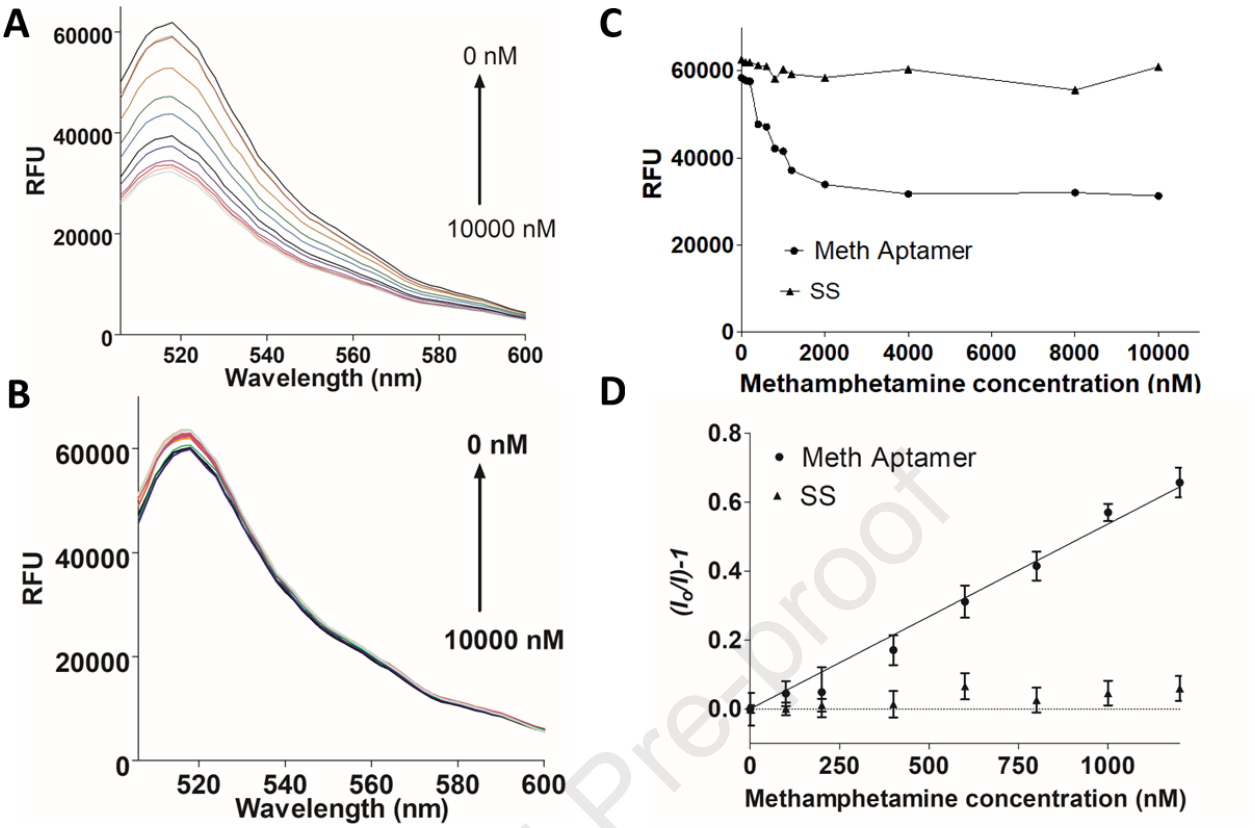

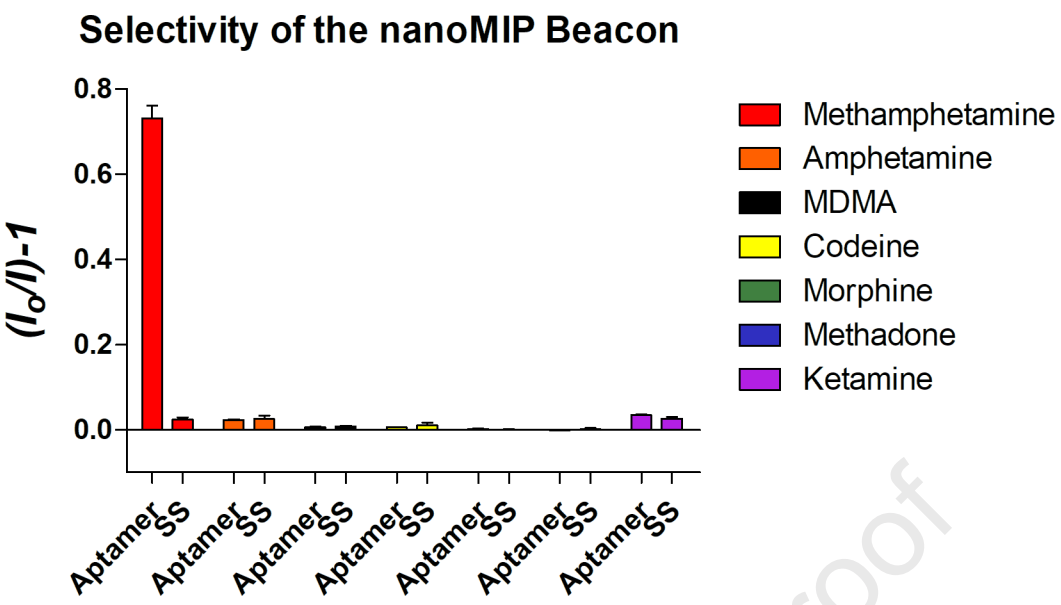

Declaration of interests

☐ The authors declare that they have no known competing financial interests or personal relationships that could have appeared to influence the work reported in this paper.

☒ The authors declare the following financial interests/personal relationships which may be considered as potential competing interests:

Jon Ashley reports financial support was provided by CAM. If there are other authors, they declare that they have no known competing financial interests or personal relationships that could have appeared to influence the work reported in this paper.